Commun Nonlinear Sci Numer Simulat 59 (2018) 375–386

Contents lists available at ScienceDirect

Commun Nonlinear Sci Numer Simulat

journal homepage: www.elsevier.com/locate/cnsns

Research paper

Initialization of a fractional order identification algorithm applied for Lithium-ion battery modeling in time domain

Achraf Nasser Eddine*, Benoît Huard, Jean-Denis Gabano, Thierry Poinot

Université de Poitiers, LIAS, 2 rue Pierre Brousse, TSA 41105, Poitiers Cedex 9 86073, France

ARTICLE INFO

Article history:
Received 21 September 2017
Revised 14 November 2017
Accepted 28 November 2017
Available online 2 December 2017

Keywords:
Fractional systems
Non integer modeling
Batteries
System identification
Parameter estimation
Nernst model
Warburg impedance

ABSTRACT

This paper deals with the initialization of a non linear identification algorithm used to accurately estimate the physical parameters of Lithium-ion battery. A Randles electric equivalent circuit is used to describe the internal impedance of the battery. The diffusion phenomenon related to this modeling is presented using a fractional order method. The battery model is thus reformulated into a transfer function which can be identified through Levenberg–Marquardt algorithm to ensure the algorithm's convergence to the physical parameters. An initialization method is proposed in this paper by taking into account previously acquired information about the static and dynamic system behavior. The method is validated using noisy voltage response, while precision of the final identification results is evaluated using Monte-Carlo method.

1. Introduction

Electrochemical cells are one of the most important devices used for generating energy from chemical reactions in many electrical systems. Batteries are composed of one or more electrochemical cells. Several kinds of batteries are distinguished by their internal chemical reactions such as Alkaline, Lead-acid, Lithium-ion and others. Lithium-ion batteries have many important properties which include high density, durability and high specific power [1]. For these reasons, they are nowadays integrated into several applications such as electric vehicles [2], spacecrafts [3] and electronic devices [4]. Accuracy of battery model is requested for these applications, hence some aspects such as chemical characteristics, thermodynamic properties and diffusion process should be considered.

Several models that differ among communities, have been developed to ensure accurate description of the internal battery behavior. Electrochemists proposed models that takes into consideration the chemical properties of the batteries. The main drawback is that it takes long characterization time which complicates their use in real time applications such as in the battery management systems [5]. Mathematicians developed some useful stochastic models although they generally lack the physical meaning [6–8]. Electrical engineers aim to describe the internal behavior of batteries using equivalent electric circuits composed of resistors, capacitors and voltage sources [9,10]. The main advantage of these methods lays in the simplicity of their simulation in different applications and their ability to reflect all internal battery phenomena.

The equivalent electric circuits made of three components in a series connection are mainly based on spectroscopic experiments. The first component is the resistance of electrolyte and connection within the cell. The second component is

* Corresponding author.
E-mail addresses: achraf.nasser.eddine@univ-poitiers.fr (A. Nasser Eddine), benoit.huard@univ-poitiers.fr (B. Huard), jean.denis.gabano@univ-poitiers.fr (J.-D. Gabano), thierry.poinot@univ-poitiers.fr (T. Poinot).

https://doi.org/10.1016/j.cnsns.2017.11.034
1007-5704/

the charge transfer impedance that corresponds to dynamics within the medium to high frequencies. The third component corresponds to the diffusion impedance whose dynamics are covering the low up to medium frequencies. Diffusion phenomenon is the most difficult process to account for considering the internal battery behavior modeling. The main three diffusion models are: Nernst, Restrictive and Semi-infinite [11]. In this paper, only Nernst diffusive model will be considered.

The main disadvantage of the spectroscopic experiments is that they are very restrictive in terms of time. Indeed, characterizing the low frequency behavior of a battery could lead to very long experiments. In order to get over this problem, links existing between frequency and time domains could be relevantly used to identify models derived from equivalent electric circuits without spectroscopy. In this paper, the proposed method is based on time domain fractional modeling. Identification results applied to thermal systems [12–14] and batteries [15,16] have shown that fractional models are highly suitable to describe the diffusion behavior. Diffusion impedance, also known as Warburg impedance, is directly simulated using a fractional impedance with only one half order integrator which is simulated using a fractional operator. The fractional model parameters are linked to the corresponding physical parameters.

Once the battery model is determined based on the fractional modeling, a gray-box model identification is required to retrieve physical battery components. Non linear identification algorithm, such as Levenberg–Marquardt could be used for this purpose. As it is an iterative algorithm, an initialization process is required to ensure the convergence of the algorithm to the real system parameters. Therefore, the more this initialization is closer to the real values, the more the algorithm will be able to converge quickly and accurately.

The objective of this paper is to present an initialization method that insures accurate convergence of the Levenberg–Marquardt algorithm. The presented method is based on a very poor *a priori* information about the impedance characteristics, and allows a convenient initialization of the model parameters which leads to a proper convergence of the identification algorithm. Simulations using noiseless data are performed in order to check the ability of the initialization procedure combined with Marquardt algorithm to obtain the impedance physical parameters. Noisy simulations are also provided in order to confirm this ability.

This paper is divided into six sections. The equivalent electric circuit battery modeling is firstly introduced in section two, then the fractional modeling and its application to the battery behavior are presented in section three. The identification algorithm and its initialization method are given in section four. In section five, the identification results are displayed and they are compared to a time domain simulator derived from this electric circuit that is described also in this section. Finally, the conclusion and perspectives of this work are presented in section six.

2. Battery electrochemical impedance model

Several models have been developed to describe the internal behavior of the electrochemical cell [17,18]. These models are used to predict the state of charge, the state of health and the global performance of the battery [19,20].

Storage and generation of electrical energy involved in batteries are governed by electrochemical processes whose dynamics can be clearly distinguished by:

- charge transfer phenomenon which corresponds to the flux of oxidizing and reducing species from one electrode to another,
- diffusive ionic mass transport through the electrolyte, whose dynamics are generally far much slower than those encountered in charge transfer process.

Electrical circuits are proposed to characterize the internal behavior of the cell. By considering the double layer capacitance corresponding to the electrical representation of the electrodes-electrolyte interface, equivalent impedance can be established using a simplified Randles circuit based on the separation of charge transfer and diffusion dynamics (Fig. 1). This circuit is extracted from the traditional Randles scheme by assuming that the diffusion time constant is one hundred times higher than the time constant related to charge transfer aspect [21,22].

The physical components used in this model are able to represent static and dynamic aspects of the electrochemical cell as follows:

* R_{ext}: electrolyte and connection resistance.
* R_{ct} : charge transfer resistance.

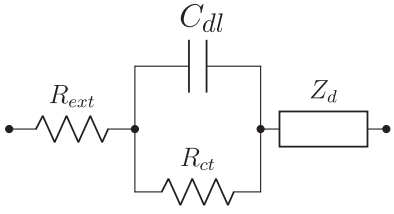

Fig. 1. Simplified Randles impedance.

* C_{dl} : double layer capacity.
* Z_d : Warburg impedance that reflects the diffusion aspect.

The $R_{ct}//C_{dl}$ circuit characterized by an impedance $Z_{ct}(s)$ represents the charge transfer phenomenon, while the global Randles equivalent impedance is defined by the equation below:

$$Z_R(s) = R_{ext} + Z_{ct}(s) + Z_d(s) \tag{1}$$

where $Z_{ct}(s) = \frac{R_{ct}}{1+\tau_{ct}s}$ and $\tau_{ct} = R_{ct}C_{dl}$ represents the time constant of the charge transfer.

Considering batteries in which Nernst diffusion phenomenon is involved [11], the diffusive impedance $Z_d(s)$ is denoted as:

$$Z_d(s) = R_d \frac{\tanh\left(\sqrt{\tau_d s}\right)}{\sqrt{\tau_d s}} \tag{2}$$

where R_d is the diffusion resistance and τ_d the diffusion time constant.

The overall impedance $Z_R(s)$ is therefore characterized by the following five physical parameters:

$$\underline{\theta}_p^T = [R_{ext}, R_{ct}, \tau_{ct}, R_d, \tau_d] \tag{3}$$

Fig. 2 shows the general pattern of Nyquist plot characteristics of the overall impedance $Z_R(jf)$ considering well separated time constants ($\tau_d \geq 1000\,\tau_{ct}$). The semi-circle obtained at high frequencies is a characteristic of impedance $Z_{ct}(jf)$. The spot at the top of the semi-circle is characterized by its real part $R_{ext} + R_{ct}/2$, its imaginary part $R_{ct}/2$ and its cut-off frequency $f_{ct} = 1/(2\pi\,\tau_{ct})$.

At lower frequencies, in the Warburg area, the Nyquist plot draws with the real part a line of 45° angle, while it turns to be a circle segment at very low frequencies which intersects the real part at $R_{ext} + R_{ct} + R_d$.

3. Battery fractional modeling

Fractional calculus has been a widely used topic in many applications such as heat transfer [12,13] and batteries [15,16]. Fractional field which is also known as non integer order presents an accurate solution for simulating diffusion behavior. In this section, Eq. (1) given in Laplace domain is approximated by a state space model in order to provide time domain data for the required identification process.

3.1. Fractional modeling of Nernst diffusion

Nernst diffusion model is simulated in this subsection using fractional order integrator. The hyperbolic tangent used in Nernst diffusion model defined in Eq. (2) can be represented using a series expansion as follows:

$$\tanh(x) = \sum_{n=1}^{\infty} \frac{2^{2n}(2^{2n}-1)B_{2n}}{2n!} x^{2n-1} \quad \text{for } |x| < \frac{\pi}{2} \tag{4}$$

where B_n are the *Bernoulli* numbers.

The low frequency approximation $Z_{d,\,lf}(s)$ can be obtained by applying this expansion on Eq. (2) :

$$Z_{d,lf}(s) = R_d\left(1 - \frac{\tau_d s}{3}\right) \tag{5}$$

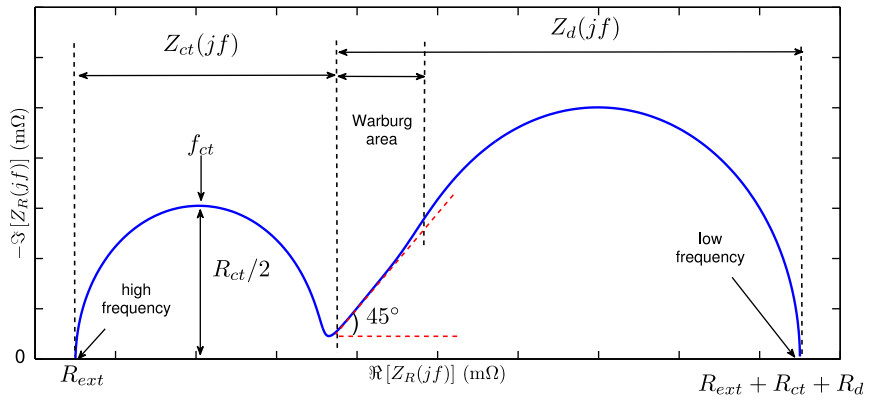

Fig. 2. Nyquist diagram of the overall impedance model (1).

3.2. Fractional operator

Fractional orders are used to accurately describe the diffusion phenomenon inside Lithium-ion batteries [23]. An operator $\mathcal{I}_n(\omega_b, s)$ is defined to characterize a fractional behavior in a frequency range defined by $[\omega_b; \omega_h]$ [24,25]:

$$\mathcal{I}_n(\omega_b, s) = \frac{\omega_b^{-n}}{s} \prod_{i=1}^{N_c} \frac{1 + \frac{s}{\omega_i'}}{1 + \frac{s}{\omega_i}} \tag{6}$$

The lowest and highest frequencies are defined as ω_b and ω_h, respectively. The lower frequency value ω_b is a parameter that should be able to adapt and limit the fractional order at low frequency. Meanwhile, the upper frequency value ω_h should be set adequately high so that it allows the operator $\mathcal{I}_n(\omega_b, s)$ to behave as a non integer integrator for the desired frequency simulations. As defined in [26], the upper frequency can be expressed using the sampling period T_s as follows:

$$\omega_h = 10 \times \frac{\pi}{T_s} \tag{7}$$

The operator $\mathcal{I}_n(\omega_b, s)$ can be simulated in time domain using the state space representation as presented in [27]. The global impedance model using fractional modeling of the diffusive part is given by:

$$Z_{Rfrac}(s) = R_{ext} + Z_{ct}(s) + Z_{dfrac}(s) \tag{8}$$

where:

$$Z_{dfrac}(s) = \frac{b_0 \mathcal{I}_{0.5}(\omega_b, s)}{1 + a_0 \mathcal{I}_{0.5}(\omega_b, s)} \tag{9}$$

The model is then defined using six parameters:

$$\underline{\theta}_R^T = [R_{ext}, R_{ct}, \tau_{ct}, a_0, b_0, \omega_b] \tag{10}$$

Therefore the fractional model used for characterizing Nernst diffusion is defined using three structural parameters:

$$\underline{\theta}_{dfrac}^T = [a_0, b_0, \omega_b] \tag{11}$$

Therefore, the asymptotic behavior $Z_{dfrac,\,lf}$ of Eq. (9) at low frequency ($\omega \ll \omega_b$) can be evaluated as follows:

$$Z_{dfrac,lf}(s) = \frac{b_0}{a_0}\left(1 - \frac{s}{a_0 \omega_b^{0.5}}\right) \tag{12}$$

The physical parameters R_d and τ_d can be obtained from the structural parameters a_0, b_0 and ω_b by considering the low asymptotic behaviors of Nernst diffusion model (Eq. (5)) and its fractional modeling (Eq. (12)):

$$\begin{cases} R_d = \dfrac{b_0}{a_0} \\ \tau_d = \dfrac{3}{a_0 \sqrt{\omega_b}} \end{cases} \tag{13}$$

4. Identification method and algorithm initialization

4.1. Introduction

In addition to the physical parameters estimation, the main goal of this section is to present an initialization process for the identification algorithm that is used to identify the impedance model given in (8). Levenberg–Marquardt identification algorithm has been widely used for solving nonlinear equations [28]. This iterative algorithm is used to identify a vector of structural parameters such as $\underline{\theta}_R$ expressed in (10). Since it is an iterative algorithm, proper initialization values are required to avoid deviated or divergent estimated results. The following subsections present an explanation on how to determine an initialization vector that is able to converge to the real parameters values.

4.2. Levenberg–Marquardt identification algorithm

Levenberg–Marquardt is a nonlinear optimization least squares method, that presents a combination between Gradient and Gauss–Newton methods [29,30]. This combination is controlled using a damping factor which allows with its high value the algorithm to act like gradient method and with its low value to act like Gauss–Newton method [31]. This algorithm represents a compromise between robustness, low sensitivity to initial values and high speed convergence specially when initialization values are close to the optimum.

Due to the non linearity model in $\underline{\theta}$, Levenberg–Marquardt algorithm is used to determine iteratively the values of $\widehat{\underline{\theta}}$ [29,32]:

$$\widehat{\underline{\theta}}_{j+1} = \widehat{\underline{\theta}}_j - \left[\left(J''_{\underline{\theta}\underline{\theta}}\right)_{\widehat{\underline{\theta}}_j} + \lambda(I_P)\right]^{-1} J'_{\widehat{\underline{\theta}}_j} \tag{14}$$

where:

- $J'_{\underline{\widehat{\theta}}_j} = -2S\underline{\varepsilon}$ is the gradient
- $\left(J''_{\underline{\theta}\underline{\theta}}\right)_{\underline{\widehat{\theta}}_j} = -2SS^T$ is the pseudo-Hessian
- λ represents the damping factor which allows switching between gradient descent method and Gauss–Newton method.
- I_P represents the Pth identity matrix.

Considering the parameters $\underline{\theta} = \underline{\theta}_R$ of the investigated model defined by Eq. (10), the sensitivity vectors are computed at each sampling time as follows:

$$\underline{\sigma}^T_{k,\underline{\theta}_R} = \left[\frac{\partial \widehat{y}_k}{\partial R_{ext}}; \frac{\partial \widehat{y}_k}{\partial R_{ct}}; \frac{\partial \widehat{y}_k}{\partial \tau_{ct}}; \frac{\partial \widehat{y}_k}{\partial b_0}; \frac{\partial \widehat{y}_k}{\partial a_0}; \frac{\partial \widehat{y}_k}{\partial \omega_b}\right] \tag{15}$$

where $\widehat{y}_k = \delta\widehat{V}_k$ is the estimated voltage response to an excitation current.

The sensitivity matrix S is therefore defined considering the whole time interval $(1 \le k \le K)$ as follows:

$$S = \left[\underline{\sigma}_{1,\underline{\theta}_R}, \ldots, \underline{\sigma}_{k,\underline{\theta}_R}, \ldots, \underline{\sigma}_{K,\underline{\theta}_R}\right] \tag{16}$$

4.3. Initialization method of Levenberg–Marquardt algorithm

4.3.1. Global presentation

Simulations are performed in time domain using pulse current of Δt duration. The initialization procedure is based on the analysis of the voltage dynamics response $R_{ext}I(t)$, $\delta V_{ct}(t)$ and $\delta V_d(t)$ to this excitation input current assuming a rectangular pulse of I_0 amplitude and starting at t_0 with a Δt duration(Fig. 3a).

The voltage response $\delta V_R(t)$ and its components due to the resistance R_{ext}, the charge transfer dynamics $\delta V_{ct}(t)$ and the diffusion dynamics $\delta V_d(t)$ are shown in Fig. 3b.

In order to exhibit the difference of dynamics due to the charge transfer impedance and the diffusion impedance, $\delta V_{ct}(t)$ and $\delta V_d(t)$ are illustrated respectively in Figs. 3c and 3-d using appropriate time scales. Δt_{ct} represents the time duration required for $\delta V_{ct}(t)$ to reach the steady state regime.

As indicated in Section 2, the only *a priori* information about the impedance characteristics is supposed to be very poor, *i.e.* the charge transfer time constant $(\tau_{ct})_{a\,priori}$ can be chosen to be as high as up to six times the exact value τ_{ct} and the diffusion time constant is supposed to respect $\tau_d \ge 100\,\tau_{ct}$.

The initialization method allows the calculation of the initial parameters $\underline{\theta}_{Rinit}$ from the voltage variation during the current pulse. This vector is divided into three parts as follows:

$$\underline{\theta}_{Rinit} = [\underline{\widehat{\theta}}_{R0}, \widehat{\omega}_{b0}, \underline{\widehat{\theta}}_{d0}] \tag{17}$$

where $\underline{\widehat{\theta}}_{R0}$ includes the electrolyte resistance $\widehat{R}_{ext}$ and the charge transfer parameters $\widehat{R}_{ct}$ and $\widehat{\tau}_{ct}$ while $\underline{\widehat{\theta}}_{d0}$ includes fractional model parameters $\widehat{a}_0$ and $\widehat{b}_0$. Each part of $\underline{\theta}_{Rinit}$ vector calculation defines a step, which will be developed during the following subsections:

1. Estimation of $\underline{\widehat{\theta}}_{R0}$ by applying Levenberg–Marquardt algorithm as a system that includes only the aforementioned three parameters.

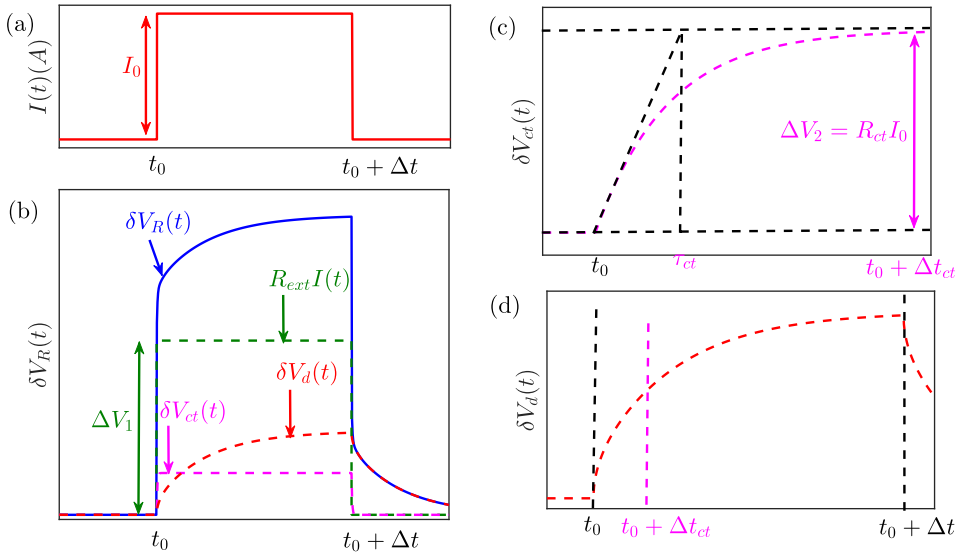

Fig. 3. Voltage dynamic response analysis to a rectangular pulse current excitation.

2. Estimation of $\widehat{\omega}_{b0}$ using results obtained from the first step.
3. Estimation of $\underline{\widehat{\theta}}_{d0}$ using the least squares method.

4.3.2. Initialization of R_{ext}, R_{ct} *and* τ_{ct}

The first step of the method starts by applying Levenberg–Marquardt algorithm to a simplified model of the impedance without including the diffusive part. This model is defined as follows:

$$Z_{R0}(s) = R_{ext0} + \frac{R_{ct0}}{1 + \tau_{ct0} s} \tag{18}$$

This simplified model is characterized by the three following parameters:

$$\underline{\theta}_{R0}^{T} = [R_{ext0}, R_{ct0}, \tau_{ct0}] \tag{19}$$

The initialization parameters of the simplified model should be calculated in order to perform the identification algorithm. Hence, the three parameters of $\underline{\theta}_{R0}$ should be initialized.

First, according to Eq. (18), the resistance R_{ext} acts as a direct transmission. For this reason, this step consists of detecting the rising edge of current signal $I(t)$. Therefore an estimation of the voltage increase ΔV_1 due to the resistance R_{ext} (Fig. 3-b) can be performed, and its initial value can be calculated by:

$$R_{ext0,init} = \frac{\Delta V_1}{I_0} \tag{20}$$

By considering the diffusion dynamics negligible with respect to the charge transfer dynamics within the time interval from t_0 to $t_0 + \Delta t_{ct}$, model $Z_{R0}(s)$ is identified using output voltage data. The value Δt_{ct} is set using *a priori* knowledge about the time constant τ_{ct} as follows:

$$\Delta t_{ct} = 3(\tau_{ct})_{a\ priori} \tag{21}$$

An estimation of the voltage variations $\delta\widehat{V}_{ct}(t)$ due to the charge transfer process is then computed as follows:

$$\delta\widehat{V}_{ct}(t) = \delta V_R(t) - R_{ext0} I(t) \tag{22}$$

Therefore, the initial value of the resistance R_{ct} is easily obtained from $\delta\widehat{V}_{ct}(t)$ considering the voltage variation at time $t_0 + \Delta t_{ct}$. At this time the steady state can be considered reached (Fig. 3c):

$$R_{ct0} = \frac{\Delta V_2}{I_0} \tag{23}$$

Using the results of Eqs. (20), (23) and Δt_{ct}, Levenberg–Marquardt algorithm is applied to identify $Z_{R0}(s)$ with the following initial vector parameter:

$$\underline{\theta}_{R0,init}^{T} = [R_{ext0,init}, R_{ct0,init}, (\tau_{ct})_{a\ priori}] \tag{24}$$

After convergence of the algorithm, estimated parameters $\underline{\widehat{\theta}}_{R0}$ will be used to continue the initialization procedure:

$$\underline{\widehat{\theta}}_{R0}^{T} = [\widehat{R}_{ext0}, \widehat{R}_{ct0}, \widehat{\tau}_{ct0}] \tag{25}$$

4.3.3. Initialization of ω_b

The main complexity of the diffusion behavior resides in the detection of its frequency boundary limit. ω_b is the parameter which guarantees the optimal transition between the first order behavior ($\omega < \omega_b$) and the half order behavior ($\omega > \omega_b$) of the diffusion impedance.

Based on different trials of ω_b initial values and its effect on the final identification algorithm results, it is concluded that the proper initialization requires the use of a value which corresponds to Warburg area where Nyquist plot exhibits a 45° line with the real part (see figure (2)). Fig. 4 shows Nyquist patterns of the overall impedance for different time constants ratio (τ_d/τ_{ct}). It is noticed that for Nyquist patterns with time constants ratio between 100 and 1000, $\omega_{ct}/10$ corresponds approximately to the upper limit frequency of Warburg area (for $\tau_d = 500\ \tau_{ct}$ and $\tau_d = 1000\ \tau_{ct}$), while for $\tau_d = 100\ \tau_{ct}$, it corresponds to a frequency within Warburg area.

Therefore, the pulsation ω_b can be initialized at one decade below the estimated charge transfer cut-off frequency:

$$\widehat{\omega}_{b0} = \frac{\widehat{\omega}_{ct0}}{10} = \frac{1}{10 \times \widehat{\tau}_{ct0}} \tag{26}$$

where $\widehat{\omega}_{ct0}$ is the estimated cutoff frequency of impedance $Z_{ct}(s)$ computed using the previous estimation of time constant $\widehat{\tau}_{ct0}$.

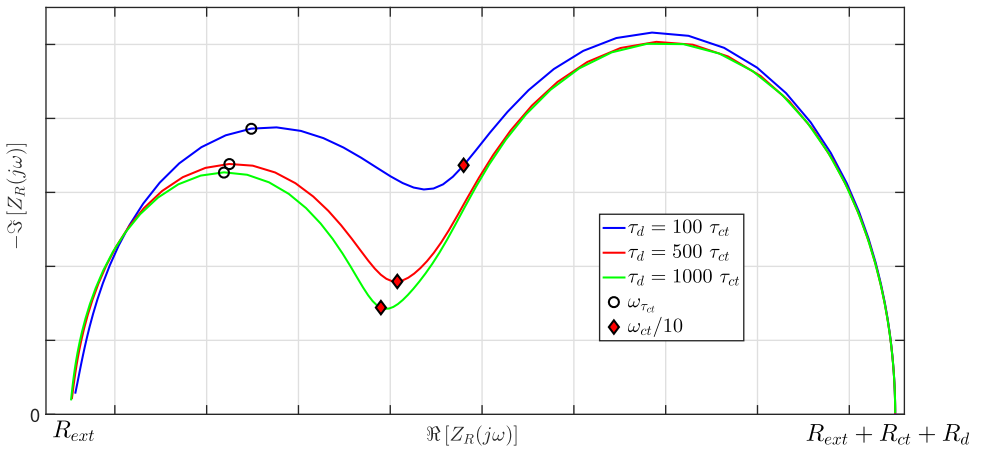

Fig. 4. Relative ω_{ct} positions at one decade according to different Nyquist patterns.

4.3.4. Initialization of b_0 *and* a_0

This step consists of determining the initial values of the fractional model $\widehat{Z}_{dfrac}(s)$ used to describe the physical model $Z_d(s)$. The determination of a_0 and b_0 can be performed using the diffusive response estimate $\delta\widehat{V}_d(t)$. Hence, this voltage diffusion dynamics are estimated as follows:

$$\delta\widehat{V}_d(t) = \delta V_R(t) - \delta\widehat{V}_{R0}(\underline{\widehat{\theta}}_{R0}, t) \tag{27}$$

where $\delta\widehat{V}_{R0}(\underline{\widehat{\theta}}_{R0}, t)$ is calculated using initial parameter estimates.

The fractional diffusion impedance model is defined by:

$$\widehat{Z}_{dfrac}(s) = \frac{\delta V_d(s)}{I(s)} = \frac{b_0\mathcal{I}_{0.5}(\omega_b, s)}{1 + a_0\mathcal{I}_{0.5}(\omega_b, s)} \tag{28}$$

where $\delta V_d(s)$ and $I(s)$ are the Laplace transformation of signals $\delta V_d(t)$ and $I(t)$. Consequently, the following representation can be obtained from Eq. (28):

$$\delta V_d(s) = -a_0\mathcal{I}_{0.5}(\omega_b, s)\delta V_d(s) + b_0\mathcal{I}_{0.5}(\omega_b, s)I(s) \tag{29}$$

Using a fixed value for the low frequency boundary ($\omega_b = \widehat{\omega}_{b0}$) of operator $\mathcal{I}_{0.5}(\omega_b, s)$, the non integer integration of signals $\delta V_d(t)$ and $I(t)$, written $\mathcal{I}_{0.5}(\omega_{b0}, s)[\delta V_d(t)]$ and $\mathcal{I}_{0.5}(\omega_{b0}, s)[I(t)]$, can be easily computed using the state space representation of operator $\mathcal{I}_{0.5}(\widehat{\omega}_{b0}, s)$. A model linear in parameters is then obtained:

$$\delta\widehat{V}_d(t) = \underline{\varphi}^T(t)\underline{\theta}_{d0} \tag{30}$$

$$\text{with}: \underline{\varphi}^T(t) = \begin{bmatrix} -\mathcal{I}_{0.5}(\widehat{\omega}_{b0}, s)[\delta V_d(t)] & \mathcal{I}_{0.5}(\widehat{\omega}_{b0}, s)[I(t)] \end{bmatrix} \quad \underline{\theta}_{d0} = \begin{bmatrix} a_0 \\ b_0 \end{bmatrix}$$

Values resulting from least squares method give the $\widehat{\theta}_{d0}$ vector presented in (17).

4.4. Accuracy of the algorithm

Accuracy of the estimated voltage value $\delta\widehat{V}_k(I, \underline{\widehat{\theta}})$ can be quantified using the adjustment fitting coefficient (FIT). This coefficient represents the percentage of the output measured voltage δV_k explained by the estimated voltage value as follows:

$$\text{FIT} = \text{MAX}\left[0, \left(1 - \sqrt{\frac{\sum_{k=1}^{K}\left(\delta V_k - \delta\widehat{V}_k(I, \underline{\widehat{\theta}})\right)^2}{\sum_{k=1}^{K}\left(\delta V_k - \delta\overline{V}_k\right)^2}}\right) \times 100\right] \tag{31}$$

where $\delta\overline{V}_k$ is the mean value:

$$\delta\overline{V}_k = \frac{1}{K}\sum_{k=1}^{K}\delta V_k \tag{32}$$

5. Identification results and discussions

In this section, simulation results of fractional modeling in time domain are presented. Initialization method and final identification results are presented first using noiseless voltage signal $\delta V(t)$ then using noisy voltage signal $\delta V^*(t)$ with a Signal to Noise Ratio (SNR) of 20 dB. Results indicate the advantage of using the proposed initialization method to obtain parameters values that converge to the requested physical parameters.

5.1. Numerical simulation

Battery impedance can be characterized in time domain using chronopotentiometric experiments. These experiments consist of applying controlled charge or discharge current steps to the battery which generates voltage variation $\delta V(t)$ across the internal impedance (Fig. 5).

Impedance $Z_R(s)$ is therefore the transfer function between the input current $I(t)$ and the output voltage variation $\delta V(t)$ which superimposes on the Open Circuit Voltage (OCV):

$$Z_R(s) = \frac{\delta V(s)}{I(s)} \tag{33}$$

where $I(s)$ and $\delta V(s)$ are Laplace transforms of signals $I(t)$ and $\delta V(t)$.

In order to generate data uncorrelated with the fractional model used to characterize the battery, an independent simulator is proposed. Thus, the electrochemical expression of the diffusive impedance $Z_d(s)$ defined in (2) is expanded using Mittag–Leffler series expansion of function $\tanh(x)$ [33]:

$$\tanh(x) = \sum_{i=1}^{\infty} \frac{2x}{x^2 + ((2n-1)\frac{\pi}{2})^2} \tag{34}$$

Therefore, using the series expansion of Eq. (34), the global impedance of the simulator can be defined as follows:

$$Z_{Rsim}(s) = R_{ext} + \underbrace{\frac{R_{ct}}{1 + R_{ct}C_{dl}s}}_{Z_{ct}(s)} + \underbrace{\sum_{n=1}^{N} \frac{R_n}{1 + R_n\frac{C_d}{2}s}}_{Z_{dsim}(s)} \tag{35}$$

with:

$$\begin{cases} R_n = \frac{8R_d}{\pi^2(2n+1)}, \\ C_d = \frac{\tau_d}{R_d} \end{cases} \tag{36}$$

This transfer function corresponds to the *RC* Foster network given in Fig. 6. Thus, the numerical simulations are performed using a linear state space representation, where $N+1$ state variables are the voltage drops across each elementary cell.

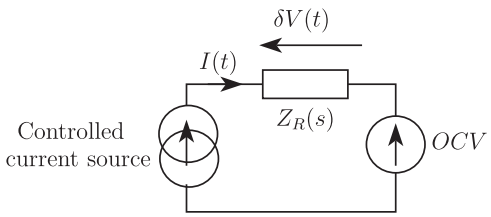

Fig. 5. Chronopotentiometry experiment principle.

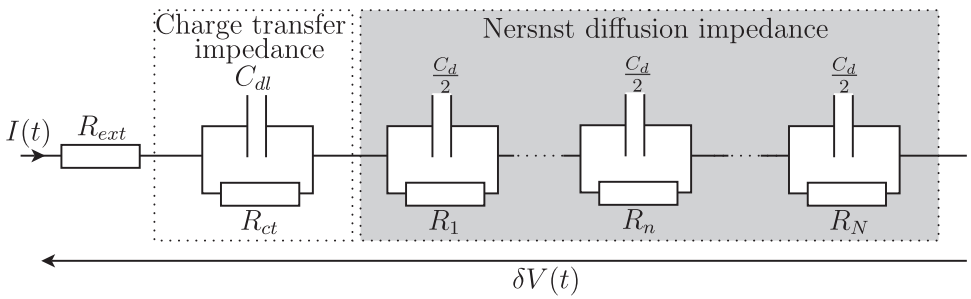

Fig. 6. *RC* Foster network used to perform numerical simulations in the time domain.

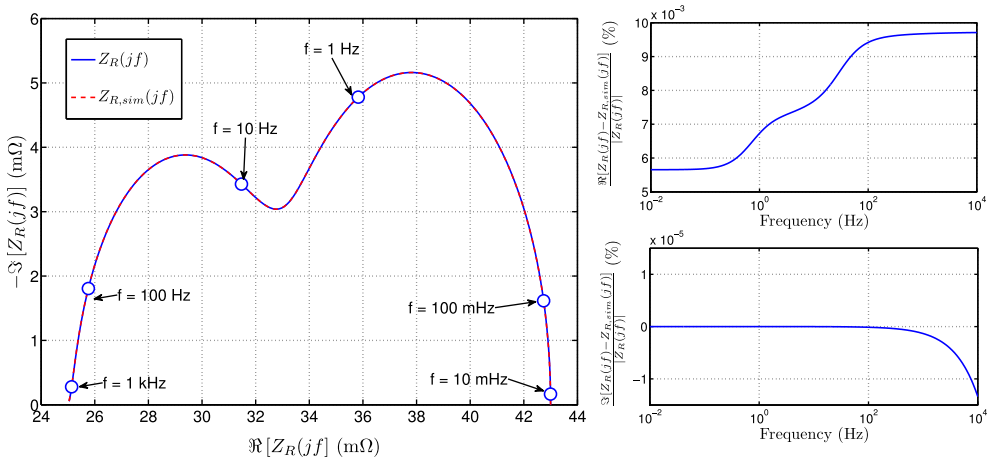

Fig. 7. Nyquist diagram of Nernst diffusion using hyperbolic tangent and the simulator with relative error of real and imaginary parts.

Therefore, the simulation of the electrochemical impedance allows to generate input and output signal characteristics define by physical parameter presented in (3). These parameters will be used to validate the fractional model used in the identification procedure :

$$\begin{cases} R_{ext} = 25\ \text{m}\Omega \\ R_{ct} = 6\ \text{m}\Omega \\ \tau_{ct} = 6.5\ \text{ms} \\ R_d = 12\ \text{m}\Omega \\ \tau_d = 650\ \text{ms} \end{cases} \tag{37}$$

Using $N = 1000$ cells[1], Fig. 7 shows that the simulator $Z_{Rsim}(s)$ is able to provide dynamic voltage responses to excitation current in the time domain quasi similar to those corresponding to the electrochemical impedance $Z_R(s)$. Indeed, the relative error between the real parts and the imaginary parts of simulator $Z_{Rsim}(jf)$ and electrochemical impedance $Z_R(jf)$ is lower than $\pm 0.01\,\%$ in the frequency band [0.1 mHz − 10 kHz].

5.2. Identification results: Noiseless signals

A simulation using noiseless voltage signal is used in order to validate the effect of the initialization method in the final convergence of the algorithm. A pulse current of 2 s duration and 3 A amplitude is applied and the sampling time is equal to 250 µs. The total duration of the current signal is 10 s. Two principle factors are evaluated in order to study their impact on the identification algorithm:

1. Influence of the $(\tau_{ct})_{a\ priori}$ initialization value.
2. Influence of the ratio between charge transfer and diffusion times constants.

5.2.1. Influence of the $(\tau_{\text{ct}})_{\text{a priori}}$ initialization value

Simulation with $\tau_d = 100\ \tau_{ct}$ demonstrated that when using *a priori* charge transfer time constant $(\tau_{ct})_{a\ priori}$ up to six times the exact value of the initialization procedure presented in Section 4.3 allows to obtain a proper convergence of Levenberg–Marquardt algorithm towards the exact physical parameters as shown in Table 1. The fractional model allows to obtain the physical parameters with an absolute estimation error lower than 2% except for the charge transfer time constant where its relative error is equal to 3.9%.

By selecting $(\tau_{ct})_{a\ priori}$ far from the exact value ($> 6\,\tau_{ct}$), the initialization procedure provides initial values so that Levenberg–Marquardt algorithm converge to parameters with a lack of physical meaning such as the estimated charge transfer time constants $\widehat{\tau}_{ct}$ which converge to negative values.

5.2.2. Influence of the ratio between charge transfer and diffusion times constants.

Another factor is evaluated which is the ratio between charge transfer and diffusion time constants (τ_d/τ_{ct}). As shown in Fig. 4, this ratio has an important impact on the battery impedance behavior. The farther each other the time constants

[1] By comparison, the fractional model needs only $N_c = 17$ cells to obtain the same accuracy which shows its parsimony.

Table 1
Final parameters Estimated Values (EV) and their Relative Errors (RE) resulting from the final Levenberg–Marquardt algorithm with $\tau_d = 100\ \tau_{ct}$ and different τ_{ct} initialization.

		$(\tau_{ct})_{a\ priori} = 6\ \tau_{ct}$		$(\tau_{ct})_{a\ priori} = 9\ \tau_{ct}$	
Physical parameters	Exact Value	EV	RE	EV	RE
R_{ext}	25 mΩ	25.01 mΩ	0.04%	25.72 mΩ	2.88%
R_{ct}	6 mΩ	6.11 mΩ	1.83%	3.74 mΩ	−37.67%
τ_{ct}	6.5 ms	6.75 ms	3.85%	−9.08ms	−239.69%
R_d	12 mΩ	11.87 mΩ	−1.08%	9.69 mΩ	−19.25%
τ_d	650 ms	656.94 ms	1.07%	419.06 ms	−35.53%

Table 2
Influence of the ratio between charge transfer and diffusion time constants on mean relative error of physical parameters resulting from the final identification algorithm.

	Relative error		
Physical parameters	$\tau_d = 100\ \tau_{ct}$	$\tau_d = 500\ \tau_{ct}$	$\tau_d = 1000\ \tau_{ct}$
R_{ext}	0.04%	0.04%	−0.04%
R_{ct}	1.83%	−0.83%	−1.00%
τ_{ct}	3.85%	2.00%	0.31%
R_d	−1.08%	0.33%	0.75%
τ_d	1.07%	−0.02%	0.27%

Table 3
Mean values, Confidence Interval (CI) and relative difference of physical parameters resulting from the initialization method.

	Initial values		
Physical parameters	Exact value	Mean ± CI	Relative difference
R_{ext}	25 mΩ	26.11 mΩ ± 0.46%	4.44%
R_{ct}	6 mΩ	8.72 mΩ ± 1.23%	45.33%
τ_{ct}	6.5 ms	11.95 ms ± 2.84%	83.85%
R_d	12 mΩ	8.18 mΩ ± 0.51%	−31.83%
τ_d	650 ms	963.04 ms ± 0.60%	48.16%

τ_d and τ_{ct} are, the more accurate the physical parameters estimates are. This is confirmed by identification results using simulations with $\tau_d = 100\ \tau_{ct}$, $\tau_d = 500\ \tau_{ct}$ and $\tau_d = 1000\ \tau_{ct}$.

Table 2 indicates proper convergence of the algorithm to the real physical parameters with different time constants ratio values. As expected, the increase of the time constants ratio decreases the relative error of charge transfer time constant from 3.9% to 0.25%. As for the other parameters, the relative errors are lower than 2%. Hence, these values prove the ability of the fractional model to obtain accurate physical parameters.

5.3. Identification results: Noisy signals

Monte-Carlo simulations are now performed in order to check the ability of initialization procedure to provide proper Levenberg–Marquardt algorithm convergence with noisy output voltage signals. Monte-Carlo method is implemented with 100 trials. Noisy signals with SNR of 20 dB are added to the voltage response $\delta V(t)$. The same excitation pulse current used with noiseless simulation is applied with a 250 µs sampling time. In the considered simulation, the ratio between time constants is set to 100 ($\tau_d = 100\ \tau_{ct}$).

The *a priori* knowledge about the charge transfer time constant is set such as $(\tau_{ct})_{a\ priori} = 5\ \tau_{ct}$. As presented in Table 3, the initialization procedure allows to obtain initial parameter of R_{ext} close to its exact value (absolute relative difference less than 5%). The charge transfer resistance and the diffusion parameters are distant from their exact values (absolute relative difference values lower then 50%). Finally, for the diffusion time constant τ_d, the initial value is faraway from its exact value with an absolute relative difference value higher than 80%. Results of the final estimation (Levenberg–Marquardt using initial parameters) presented in Table 4 indicate that all parameters are able to converge to their exact value with a relative difference less than 3.1%. Hence, for R_{ext} and diffusion parameters the absolute relative error values are lower than 2%. Taking into consideration simulation results for noiseless signal presented in Table 2, it can be noticed that Monte-Carlo results can be improved with other simulations with $\tau_d > 100\,\tau_{ct}$. These values prove the interest of implementing the initialization method which therefore guarantees the convergence of the identification algorithm towards accurate physical parameters estimates.

Table 4
Mean values, Confidence Interval (CI) and relative difference of physical parameters resulting from the final estimation of the identification algorithm.

	Final values		
Physical parameters	Exact value	Mean ± CI	Relative difference
R_{ext}	25 mΩ	25.01 mΩ ± 0.40%	0.04%
R_{ct}	6 mΩ	6.18 mΩ ± 2.06%	3.00%
τ_{ct}	6.5 ms	6.70 ms ± 2.71%	3.08%
R_d	12 mΩ	11.81 mΩ ± 1.01%	−1.58%
τ_d	650 ms	661.77 ms ± 1.00%	1.81%

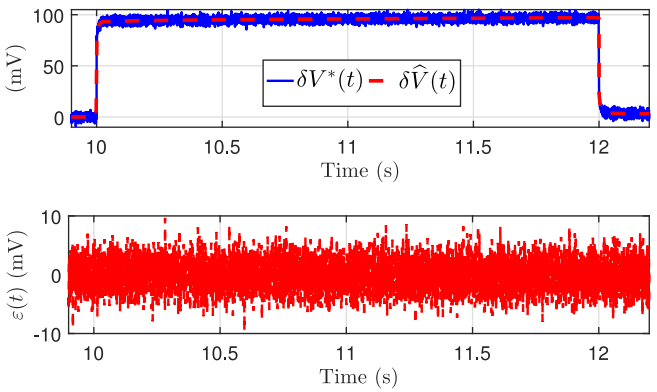

Fig. 8. Noisy simulation results of identification based on the time domain characterization.

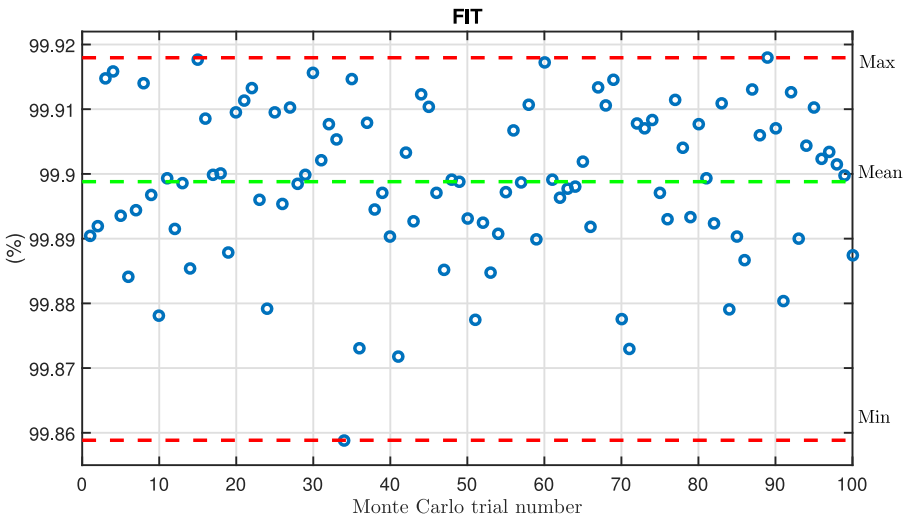

Fig. 9. Results of FIT between actual measurement voltage response and estimated voltage values for the 100 measurements.

Fig. 8 represents a comparison between noisy voltage response $\delta V^*(t)$ and estimated voltage $\delta\widehat{V}(t)$ resulting from the identification algorithm. Curves clearly show the ability of the fractional model to converge to the real voltage response of the battery even with SNR of 20 dB. Hence it is observed that the identification using the presented initialization method is able to converge and the residual voltage response indicates the accurate convergence in time domain. Fig. 9 presents the results of FIT between actual measured voltage response $\delta V^*(t)$ and estimated voltage response $\delta\widehat{V}(t)$ for the 100 measurements. It is shown that values of FIT are greater than 99.85% which indicate the validity of using the fractional method to identify the internal impedance of the battery.

6. Conclusion

An initialization method for identification algorithm is proposed in this paper in order to accurately calculate the physical parameters of Lithium-ion battery. Parameters are calculated from voltage response in time domain. Modified Randles circuit

is used to model the internal impedance behavior of the battery. The diffusion impedance is characterized using fractional order model.

The ability of the fractional model to properly estimate the impedance physical parameters has been tested using an independent simulation model based on *RC* Foster network. Thanks to the proposed initialization method which requires very few information about the order of magnitude of the charge transfer time constant value, results using Monte-Carlo method and noisy voltage responses show accurate convergence of Levenberg–Marquardt algorithm.

This study could be implemented on a real bench in further works which allows the calculation of the battery parameters in time domain that has a real advantage in terms of time compared to spectroscopic experiments.

References

[1] Lu L, Han X, Li J, Hua J, Ouyang M. A review on the key issues for lithium-ion battery management in electric vehicles. J Power Sources 2013;226:272–88. doi:10.1016/j.jpowsour.2012.10.060.

[2] Farmann A, Sauer DU. A comprehensive review of on-board state-of-available-power prediction techniques for lithium-ion batteries in electric vehicles. J Power Sources 2016;329:123–37. doi:10.1016/j.jpowsour.2016.08.031.

[3] Bugga R, Smart M, Whitacre J, West W. Lithium ion batteries for space applications. In: 2007 IEEE Aerospace Conference; 2007. p. 1–7. doi:10.1109/AERO.2007.352728.

[4] Gao L, Liu S, Dougal RA. Dynamic lithium-ion battery model for system simulation. IEEE Trans Compon Packag Technol 2002;25(3):495–505. doi:10.1109/TCAPT.2002.803653.

[5] Newman J, Thomas KE, Hafezi H, Wheeler DR. Modeling of lithium-ion batteries. J Power Sources 2003;119:838–43. doi:10.1016/S0378-7753(03)00282-9. Selected papers presented at the 11th International Meeting on Lithium Batteries;

[6] Pascoe PE, Anbuky AH. VRLA battery discharge reserve time estimation. IEEE Trans Power Electron 2004;19(6):1515–22. doi:10.1109/TPEL.2004.836680.

[7] Chiasserini CF, Rao RR. Energy efficient battery management. IEEE J Sel Areas Commun 2001;19(7):1235–45. doi:10.1109/49.932692.

[8] Chen M, Rincon-Mora GA. Accurate electrical battery model capable of predicting runtime and I-V performance. IEEE Trans Energy Convers 2006;21(2):504–11. doi:10.1109/TEC.2006.874229.

[9] Do DV, Forgez C, Benkara KEK, Friedrich G. Impedance observer for a li-ion battery using Kalman filter. IEEE Trans Veh Technol 2009;58(8):3930–7. doi:10.1109/TVT.2009.2028572.

[10] Abu-Sharkh S, Doerffel D. Rapid test and non-linear model characterisation of solid-state lithium-ion batteries. J Power Sources 2004;130(1):266–74. doi:10.1016/j.jpowsour.2003.12.001.

[11] Diard J-P, Gorrec BL, Montella C. Handbook of Electrochemical impedance spectroscopy.

[12] Gabano J-D, Poinot T. Fractional identification algorithms applied to thermal parameter estimation. IFAC Proc Vol 2009;42(10):1316–21. doi:10.3182/20090706-3-FR-2004.00219.

[13] Gabano J-D, Poinot T. Fractional modelling and identification of thermal systems. Signal Process 2011;91(3):531–41. doi:10.1016/j.sigpro.2010.02.005. Advances in Fractional Signals and Systems

[14] Kanoun H, Gabano J-D, Poinot T. Ultracapacitor identification using continuous LPV fractional modelling. IFAC Proc Vol 2012;45(16):1073–8. doi:10.3182/20120711-3-BE-2027.00034.

[15] Sabatier J, Merveillaut M, Francisco JM, Guillemard F, Porcelatto D. Lithium-ion batteries modeling involving fractional differentiation. J Power Sources 2014;262:36–43. doi:10.1016/j.jpowsour.2014.02.071.

[16] Wang B, Li SE, Peng H, Liu Z. Fractional-order modeling and parameter identification for lithium-ion batteries. J Power Sources 2015;293:151–61. doi:10.1016/j.jpowsour.2015.05.059.

[17] Kuhn E, Forgez C, Lagonotte P, Friedrich G. Modelling Ni-mh battery using cauer and foster structures. J Power Sources 2006;158(2):1490–7. doi:10.1016/j.jpowsour.2005.10.018.

[18] Karden E, Buller S, Doncker RWD. A method for measurement and interpretation of impedance spectra for industrial batteries. J Power Sources 2000;85(1):72–8. doi:10.1016/S0378-7753(99)00385-7.

[19] Huet F. A review of impedance measurements for determination of the state-of-charge or state-of-health of secondary batteries. J Power Sources 1998;70(1):59–69. doi:10.1016/S0378-7753(97)02665-7.

[20] Zhong Q, Zhong F, Cheng J, Li H, Zhong S. State of charge estimation of lithium-ion batteries using fractional order sliding mode observer. ISA Trans 2017;66:448–59. doi:10.1016/j.isatra.2016.09.017.

[21] Gagneur L, Driemeyer-Franco A, Forgez C, Friedrich G. Modeling of the diffusion phenomenon in a lithium-ion cell using frequency or time domain identification. Microelectron Reliab 2013;53(6):784–96. doi:10.1016/j.microrel.2013.03.009.

[22] Gabano J-D, Poinot T, Huard B. Bounded diffusion impedance characterization of battery electrodes using fractional modeling. Commun Nonlinear Sci Numer Simul 2017;47:164–77. doi:10.1016/j.cnsns.2016.11.016.

[23] Montaru M, Pelissier S. Frequency and temporal identification of a Li-ion polymer battery model using fractional impedance. IFP Int Conf 2009;65(1):67–78. doi:10.2516/ogst/2009056.

[24] Benchellal A, Poinot T, Trigeassou J-C. Approximation and identification of diffusive interfaces by fractional models. Signal Process 2006;86(10):2712–27. doi:10.1016/j.sigpro.2006.02.025.

[25] Poinot T, Trigeasssou J-C, Lin J. Parameter estimation of fractional models: application to the modeling of diffusive systems. IFAC Proc Vol 2002;35(1):319–24. doi:10.3182/20020721-6-ES-1901.00464.

[26] Gabano J-D, Poinot T, Kanoun H. LPV continuous fractional modeling applied to ultracapacitor impedance identification. Control Eng Pract 2015;45:86–97. doi:10.1016/j.conengprac.2015.09.001.

[27] Poinot T, Trigeassou J-C. A method for modelling and simulation of fractional systems. Signal Process 2003;83(11):2319–33. Fractional Signal Processing and Applications; doi: 10.1016/S0165-1684(03)00185-3.

[28] Cui M, Zhao Y, Xu B, wei Gao X. A new approach for determining damping factors in Levenberg–Marquardt algorithm for solving an inverse heat conduction problem. Int J Heat Mass Transf 2017;107:747–54. doi:10.1016/j.ijheatmasstransfer.2016.11.101.

[29] Marquardt DW. An algorithm for least-squares estimation of nonlinear parameters. J Soc Ind Appl Math 1963;11(2):431–41. doi:10.1137/0111030.

[30] Suri FM. Signal classification using bayesian regularization and levenberg-marquardt algorithm. In: 2017 IEEE International Conference on Signal Processing, Informatics, Communication and Energy Systems (SPICES); 2017. p. 1–6. doi:10.1109/SPICES.2017.8091315.

[31] Dkhichi F, Oukarfi B, Fakkar A, Belbounaguia N. Parameter identification of solar cell model using Levenberg–Marquardt algorithm combined with simulated annealing. Sol Energy 2014;110:781–8. doi:10.1016/j.solener.2014.09.033.

[32] Franchois A, Pichot C. Microwave imaging-complex permittivity reconstruction with a Levenberg–Marquardt method. IEEE Trans Antennas Propag 1997;45(2):203–15. doi:10.1109/8.560338.

[33] Kuhn E, Forgez C, Friedrich G. Modeling diffusive phenomena using non integer derivatives. Eur Phys J Appl Phys 2004;25(3):183–90. doi:10.1051/epjap:2004009.